Structural Changes in Thermally Induced Phase Transitions of Uniaxially Oriented δ_e Form of Syndiotactic Polystyrene Investigated by Temperature-Dependent Measurements of X-ray Fiber Diagrams and Polarized Infrared Spectra

E. Bhoje Gowd, Naoya Shibayama, and Kohji Tashiro*

Department of Future Industry-oriented Basic Science and Materials, Graduate School of Engineering, Toyota Technological Institute, Tempaku, Nagoya 468-8511, Japan

Received July 22, 2006; Revised Manuscript Received September 15, 2006

ABSTRACT: The empty δ (δ_e) form of uniaxially oriented syndiotactic polystyrene (sPS) was obtained by extracting the solvent molecules from the δ form of the sPS−solvent complex in acetone and methanol. The X-ray fiber diagrams of the δ_e form of different solvents like chloroform, toluene, and benzene were found to be appreciably different from each other, probably reflecting the difference in the cavity size after solvent evaporation. Temperature dependence of the X-ray fiber diagram has been measured successfully starting from the uniaxially oriented δ_e form at various temperatures for the first time. It has been found that the δ_e form transforms to the intermediate form transiently before transforming into the γ form. Temperature-dependent polarized FTIR spectra were measured also for the uniaxially oriented δ_e sample derived from the sPS and chloroform complex. The infrared band intensity characteristic of the T_2G_2 conformation was found to change drastically in the course of transition from the δ_e to the intermediate phase and to the γ phase. On the basis of the X-ray diffraction profile and infrared spectra, the intermediate form is speculated to take the structure of disordered chain packing probably due to the empty cavities present in the original δ_e form. Thermal data showing an endotherm followed by an exotherm during the transition can be interpreted reasonably using such order-to-disorder-to-order transitions among the δ_e, intermediate, and γ forms.

Introduction

Syndiotactic polystyrene (sPS) exhibits the various types of crystal modifications with the different molecular conformations as well as the different chain-packing structures depending on the preparation conditions.[1−24] The application of external condition, e.g., temperature, solvent atmosphere, etc., causes quite complicated phase transitions.[1−24] The α and β forms with all-trans planar-zigzag (T_4) conformation are commonly obtained by thermal crystallization procedures.[3−7] The α form is obtained by cooling the melt rapidly, while the β form can be obtained by cooling the melt slowly.[3−7] They are further classified into the disordered forms (α′ and β') and the ordered forms (α″ and β'').[3−7] A mesophase of all-trans planar-zigzag conformation was also reported, which can be obtained by stretching the amorphous sample around the glass transition temperature.[8] The δ form having helical conformation [$-(T_2G_2)_2-$] can be obtained by supplying organic solvent molecules to the glassy sample: this form is a complex between the polymer and the solvent molecules.[1,2,9,10,21−23] Annealing or heating the δ form results in the formation of γ form by purging away the solvent molecules.[9−17] The γ form is solvent-free, and the T_2G_2 chains are packed closely in the crystal lattice. The γ form can be obtained also by dipping the glassy sample into solvents like acetone,[14,18] supercritical CO_2,[19] or bulky molecules which are too big to be enclosed as a guest of sPS clathrate phase.[20]

Phase transformation among these many crystal modifications of sPS were widely studied by using various techniques including X-ray and electron diffractions,[9−13,24,25] infrared and Raman spectroscopy,[14,26−29] solid-state NMR,[30,31] and energy calculations.[32] In particular, the in-situ measurements of X-ray diffraction and infrared spectra during heating process were made for the δ form of sPS with different solvent complexes to understand the phase transition mechanisms.[13,14] The δ form transforms to the γ form above 100 °C. The γ form transforms to the α form around 190 °C. The transition from δ to γ form depends on the relative amount of solvent present in the system.[13]

In addition to the above-mentioned crystal forms (δ, γ, α, and β), we know another peculiar form, the empty δ (δ_e) form. The δ_e form can be obtained by extracting the solvent molecules from the δ form in acetone and further rinsing in methanol or by extracting the δ form in supercritical CO_2.[11,17,33,34] The δ_e form also retains the helical structure similar to the δ and γ forms but with the cavities which had been occupied by solvent molecules.[11,16] The cavities are of angstrom size and are considered to be useful for the separation of solvent molecules of a particular size from the mixture of solvents.[35,36] This material is now used as a molecular filter for the purification of water and air and also in the field of chemical separation engineering.[35,36] From such an industrial application also, it is important to understand the structural changes of the δ_e form during heating. For example, we may have the following problems about the δ_e form: What is the role of cavities in the thermally induced transition from δ_e to γ phase? How are the cavities eliminated during this transition? Is there any intermediate phase in this transition process? Manfredi et al.[11,37] made the thermal treatment of the δ_e form and reported a mesophase with helical conformation. In their studies, unfortunately, the δ_e samples used were unoriented, and the discussion was more or less qualitative. Besides, the X-ray diffraction profiles reported were measured at room temperature for the samples annealed at higher temperatures. To clarify the phase transition behavior of the δ_e form more clearly, we need to carry out the in-situ measurement during the heating process.

In the present paper, we will report the structural changes during heating of the uniaxially oriented δ_e form on the basis

10.1021/ma061659d CCC: $33.50
Published on Web 10/26/2006

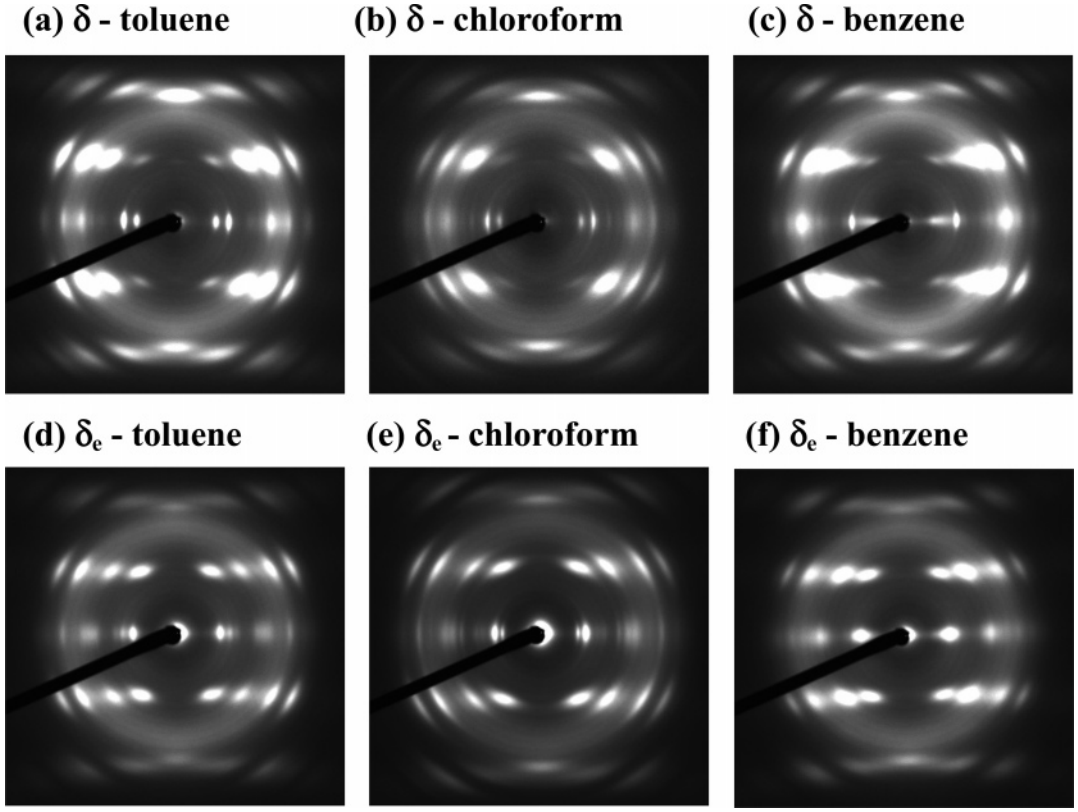

Figure 1. X-ray fiber diagrams of the sPS δ forms including (a) toluene, (b) chloroform, and (c) benzene and the corresponding emptied δ (δ_e) forms of (d) toluene, (e) chloroform, and (f) benzene.

of the X-ray diffraction and polarized infrared spectral data. We could successfully measure the X-ray fiber diagrams for uniaxially oriented δ_e form at various temperatures for the first time. The reason why the uniaxially oriented samples were used here is that the transition behavior can be clarified much better by separating the equatorial and layer line reflections. At the same time, we compared the X-ray fiber diagrams of the δ_e samples obtained from the different sPS−solvent complexes. In the second part of the paper, we will describe the change in the polarized infrared spectra during heating of the uniaxially oriented δ_e film, which may give us useful information about the intermolecular interactions as well as the chain conformation. To our knowledge, no article has appeared on the in-situ measurements of the uniaxially oriented δ_e form by using X-ray diffraction and polarized infrared spectra. We believe that the present data should make a significant contribution to better understanding of the essential features of the δ_e form, a peculiar and industrially important crystal phase of sPS.

Experimental Section

Samples. sPS pellets (M_w = 272 000, M_w/M_n = 2.28) were kindly supplied by Idemitsu Petrochemical Co., Ltd. The glassy samples were prepared by quenching the melt into ice water. A small piece of rectangular shape was cut out of the amorphous strip and stretched by about 5 times the original length above the hot plate around the glass transition temperature (97 °C). These uniaxially oriented samples were dipped in different solvents like chloroform, toluene, and benzene for 2 days at ambient temperature to obtain the δ form, where no shrinkage occurred about the sample length. The samples removed from solvents were kept at ambient temperature until they became perfectly dry. The δ_e form was obtained by refluxing the δ form samples in acetone for 15 h followed by being refluxed in methanol for 8 h to remove the residual acetone. The absence of solvent molecules in the δ_e form was confirmed by thermogravimetric analysis (TGA) measurements. A similar method was followed to prepare thin films for FTIR studies.

Measurements. *X-ray Diffraction Studies.* The oriented δ_e form was set into a brass-block heater for the X-ray diffraction measurement. This heater was set on a goniometer head of the X-ray diffraction apparatus. The fiber diagrams were recorded using an imaging plate system DIP 1000 (MAC Science Co. Japan) with graphite-monochromatized Cu Kα line as an incident X-ray beam. The X-ray fiber diagrams were recorded during the heating process.

FTIR Studies. The infrared spectra were measured with a Varian FTS 7000 series FT-IR spectrometer. The sample was sandwiched between a pair of KBr plates and then set to a homemade heating cell. The infrared spectral measurement was made at a resolution power 1 cm^{-1}. The IR polarization measurements were made using a KRS-5 wire grid polarizer. Two successive IR measurements, with parallel and perpendicular polarizations of the electric vector with respect to the draw direction of the specimen, were performed at every constant temperature during heating.

DSC Measurements. The DSC thermograms were measured in the heating process by using a differential scanning calorimeter TA Instruments DSC Q1000 under a nitrogen gas atmosphere at the rate of 10 °C/min.

Results and Discussion

Comparison of the δ_e Form of sPS from Different Solvent Complexes. The X-ray fiber diagrams of uniaxially oriented δ form containing chloroform, toluene, and benzene are given in parts a, b, and c of Figure 1, respectively. To extract the solvent from the δ form, the δ form samples were boiled in hot acetone and further in hot methanol, giving the completely emptied δ (δ_e) form. In the crystal lattice of the δ_e form, vacant spaces are kept which were originally occupied by the solvent molecules in the δ form. The X-ray fiber diagrams of the corresponding δ_e form are given in parts d, e, and f of Figure 1, respectively. Figure 2 gives the equatorial line profile of the

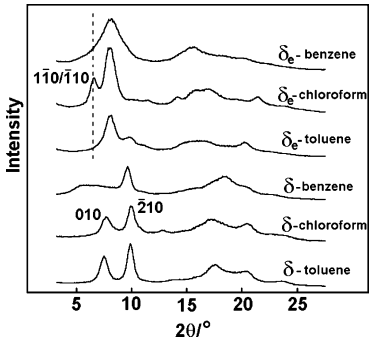

Figure 2. Comparison of the equatorial profile estimated from the X-ray fiber diagrams shown in Figure 1.

various samples, which are evaluated from the X-ray fiber diagrams shown in Figure 1. As already pointed out, the patterns of the δ form are slightly different, and the variation in the peak positions and intensities indicates that the unit cell dimensions depend on the nature and amount of the solvent trapped in the crystal lattice.[2,9] After the solvent extraction from the δ form, major changes in the X-ray fiber patterns are noticed in the intensities of the two equatorial reflections corresponding to the 010 and $\bar{2}$10 reflections, as seen in Figure 2. The $\bar{2}$10 reflection at $2\theta = 10.2°$, which is strong in the δ form, almost disappears in the δ_e form, whereas the reflection corresponding to the 101 and $\bar{1}$11 on the first layer line is very weak in the δ form and becomes very strong in the δ_e form. These observations are in good agreement with the reported results.[38] However, the comparison of X-ray diffraction data between the δ_e forms with different solvent complexes is missing in the literature. The δ_e forms derived from the different solvent complexes are expected to show difference in the X-ray diffraction pattern due to the difference in shape and volume of the cavities in the crystal lattice. As seen in Figures 1d−f and 2, the X-ray diffraction patterns of the δ_e form exhibit apparently similar pattern with the small differences in the low 2θ region on the equatorial line. The patterns of the δ_e form of toluene and benzene are almost similar to the slight variation in the peak positions and intensities whereas the chloroform gives a new reflection at $2\theta = 6.6°$ on the equatorial line. We could index this reflection to $1\bar{1}0/\bar{1}10$. It is worth mentioning here that the reflections of the δ_e form of toluene are assigned to a monoclinic unit cell with a space group $P2_1/a$, in accordance with the systematic absence of $hk0$ reflections with $h = 2n + 1$.[38] However, the new reflection ($1\bar{1}0/\bar{1}10$) observed here does not satisfy the systematic rule, suggesting that the lattice symmetry might be lowered from $P2_1/a$ due to some disorder in molecular conformation or chain-packing mode. No such reflection at $2\theta = 6.6°$ was observed for δ_e form of sPS/toluene or sPS/benzene complexes. Anyway, for deeper understanding, the detailed study of crystal structure of the δ_e form of sPS and chloroform complex is needed.

To verify that the new reflection observed in the case of δ_e form of sPS and chloroform complex corresponds to the δ_e form, we measured the temperature dependence of the X-ray fiber diagram, the details of which will be discussed in the next section. It is worth mentioning here that Yoshioka et al.[16] showed the common infrared spectra characteristic of the δ_e form irrespective of the solvent used for crystallization: a pair of bands at 607.6 and 601.9 cm^{-1}. The infrared band positions of the δ_e form may be determined in an approximation by intramolecular interaction of chains separated by the empty spaces of solvent molecules and are modified only slightly by weak interactions between the distant chains.[16]

Thermally Induced Phase Transitions of Uniaxially Oriented δ_e Form. Figure 3 shows the X-ray fiber diagrams at different temperatures starting from the δ_e form of sPS and chloroform complex. The change in the equatorial pattern

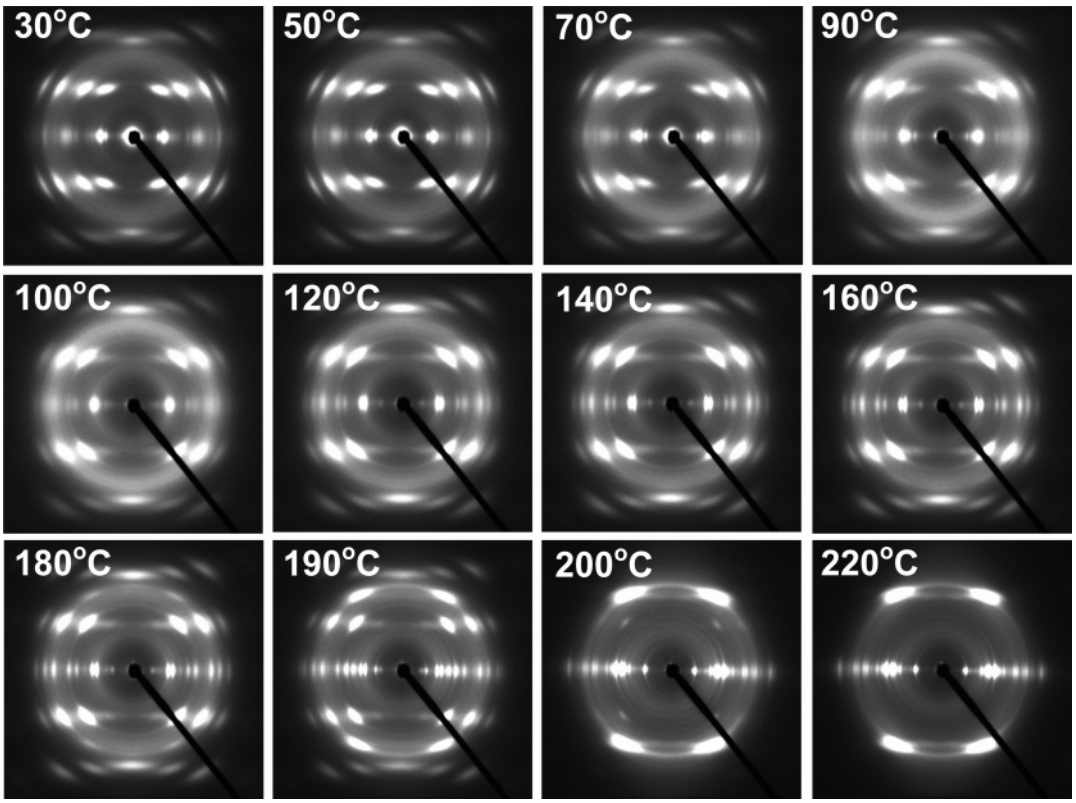

Figure 3. Temperature dependence of the X-ray fiber diagram taken for the uniaxially oriented δ_e form of sPS/chloroform complex in the heating process.

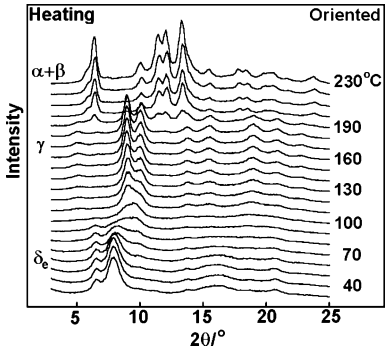

Figure 4. Temperature dependence of X-ray diffraction profile on the equatorial line of the δ_e form derived from the sPS/chloroform complex.

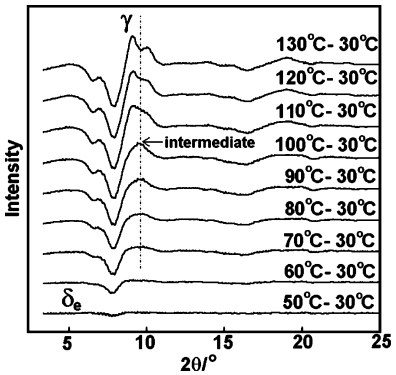

Figure 5. Equatorial profiles obtained by subtracting the equatorial profile of high-temperature patterns (70−120 °C) from the room-temperature pattern (30 °C).

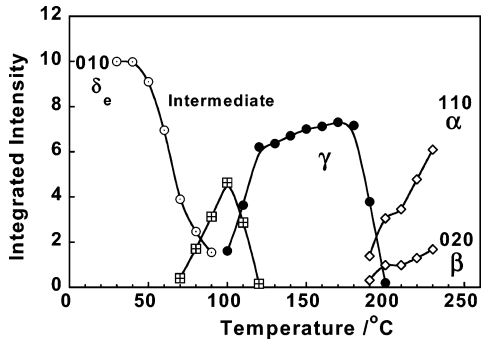

Figure 6. Temperature dependence of the integrated intensity of the reflections at $2\theta = 8.0°$ (δ_e), 9.6° (intermediate), 9.1° (γ), 6.5° (α), and 6.0° (β) evaluated from Figure 4.

evaluated from fiber diagram in the heating process is shown in Figure 4. During transition from the initial δ_e form to the γ form, we noticed the appearance of a new X-ray pattern in the temperature range 70−100 °C, which was different from those of the δ_e and γ forms. To clarify this situation, we subtracted the equatorial profile of high-temperature patterns (60−130 °C) from the room-temperature pattern (30 °C), as shown in Figure 5. An increase in downward peaks corresponds to the disappearance of the δ_e form. The upward peaks in the 120−130 °C region corresponds to the γ form. The broad upward peak in the 70−120 °C region is due to the new phase. By referring to this, we performed the curve deconvolution for the diffraction profiles given in Figure 4, and the results are shown in Figure 6. The 010 reflection of the δ_e form at $2\theta = 8.0°$ started to decrease its intensity at 70 °C and vanished at 100 °C. Simultaneously, a new characteristic reflection appeared at about $2\theta = 9.6°$ at 70 °C, and the intensity of this reflection increased up to 100 °C. But the intensity started decreasing above 100 °C and disappeared completely at 120 °C. Above 120 °C the other pattern can be detected, which corresponds to that of the γ form.

The new reflection detected in the temperature region of 70−120 °C is different from those of the δ_e and γ forms as pointed out above. This reflection might correspond to the reflection at $2\theta = 10°$ observed for the unoriented δ_e sample as reported by Manfredi et al.[11,37] They ascribed this new reflection to "helical" mesomorphic phase. Since the detailed structural analysis of this new form has not yet been made, however, it may be better to use simply the term "intermediate phase" at present.

In Figure 3, the 2-D X-ray fiber patterns observed in the temperature region 70−120 °C shows the halo-like scatterings, the intensity of which is intense at 100 °C where the intermediate phase shows its maximum contribution. These results reflect the appearance of more or less disordered chain aggregation state on the path of transition from δ_e to γ form, and the intermediate form detected during this transition process is speculated to take the disordered structure, although we do not know definitely what type of disordering occurs in this phase.

The transition behavior from the δ to γ form was investigated by Gowd et al.[13] by performing the temperature-dependent X-ray diffraction measurements during the heating process starting from the complexes with different amounts of different solvent molecules trapped in the crystal lattice. Yoshioka et al.[15] measured the infrared spectra on the path of transition from δ to γ form for the complexes of toluene, chloroform, or benzene. These two papers showed that the δ form transforms to the γ form immediately once the solvent molecules are evaporated and that the transition occurs between only these two crystalline phases without appearance of any such intermediate phase as observed in the case of the δ_e form. It means that the empty cavities present in the δ_e form are responsible for the generation of such an intermediate form. It is speculated that the molecular chains in the δ_e form are collapsed above 70 °C because of the presence of the cavities, leading to an intermediate phase of the disordered structure. In such a way all the cavities are erased, and the whole structure changed to the γ form. As the temperature increased further, the reflections of the γ form decreased steeply in a narrow temperature range of 190−200 °C and those of the α (β) forms increased instead, as shown in Figures 3 and 4. The details of the crystalline transition from γ to α (β) forms will be discussed in a separate paper.

To further understand the phase transition behavior with infrared spectroscopy, we carried out the temperature-dependent polarized infrared measurements of the uniaxially oriented δ_e sample of sPS and chloroform complex. Recently, Yoshioka et al.[16] reported the infrared frequency region sensitive to the chain-packing mode in the crystalline forms of sPS (δ, δ_e, and γ) having the same chain confirmation. We can expect to see the differences between different crystalline forms in the frequency region 450−650 cm^{-1}. Figure 7a shows the temperature dependence of polarized infrared spectra starting from the δ_e form of sPS and chloroform complex in the frequency region 450−620 cm^{-1}. The vibrational frequency and integrated intensity of the bands at 502 and 572 cm^{-1} were evaluated through the spectral deconvulation method and were plotted against temperature, as shown in Figure 7b. As the temperature increased, the bands characteristic of the δ_e form decreased in intensity, and the spectra changed to those of the γ form. No bands intrinsic of the intermediate form appeared on the way of transition from δ_e to γ form. However, the bands at 502 and 572 cm^{-1} corresponding to the T_2G_2 conformation were observed to decrease their integrated intensity in the temperature

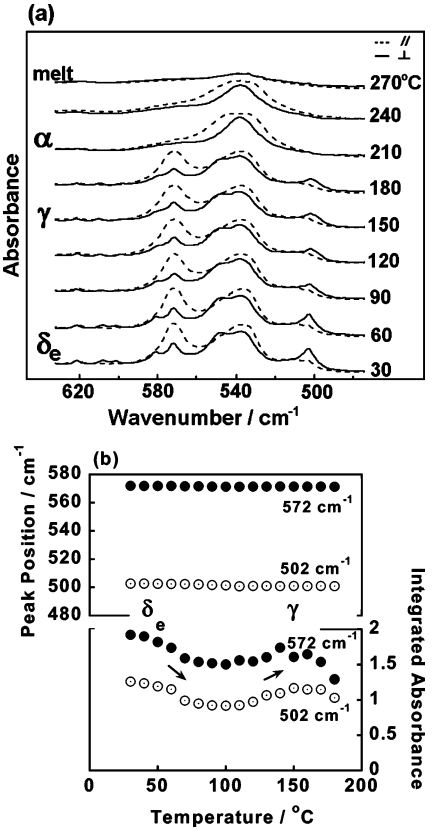

Figure 7. Temperature dependence of (a) the polarized infrared spectra in the frequency region 450−600 cm^{-1} and (b) the peak position and absorbance estimated for the bands characteristic of the δ_e and γ forms starting from the δ_e sample of sPS and chloroform complex. In (a) the solid and broken lines indicate the perpendicular and parallel band components with respect to the draw direction, respectively. Integrated absorbance is estimated for the perpendicular band component.

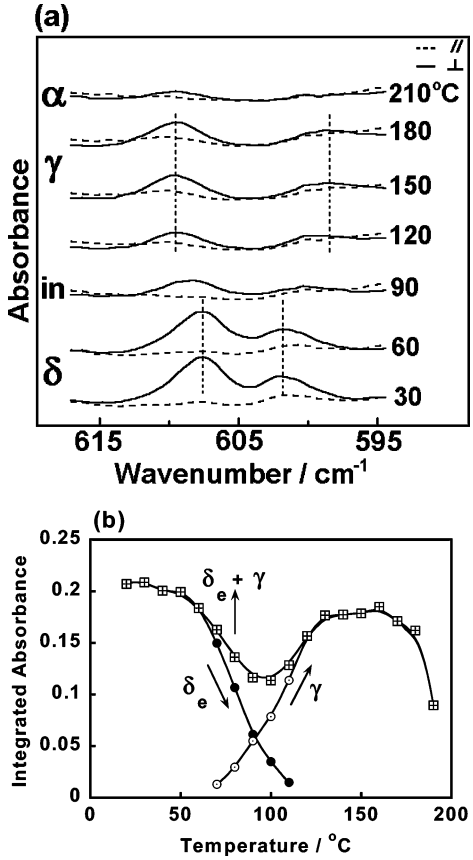

Figure 8. Temperature dependence of (a) the polarized infrared spectra in the frequency region 595−615 cm^{-1} and (b) the absorbance estimated for the bands characteristic of the δ_e and γ forms starting from the δ_e sample of sPS and chloroform complex. In (a) the solid and broken lines indicate the perpendicular and parallel band components with respect to the draw direction, respectively. Integrated absorbance is estimated for the perpendicular band component.

region 70−120 °C during the δ_e to γ transition and then increased again when the γ form appeared perfectly. This observation is essentially the same as that reported by Manfredi et al.,[11] although they measured the unpolarized infrared spectra for the unoriented sample. As the temperature increased further, the bands of the γ form decreased steeply in a narrow temperature range of 190−200 °C and those of the α form increased instead, as shown in Figure 7a. The α bands disappeared above 270 °C due to the melting of the sample. Figure 8a shows the temperature dependence of polarized infrared spectra in the frequency region 595−615 cm^{-1} starting from the δ_e form of sPS and chloroform complex. The integrated absorbance was plotted against temperature in Figure 8b. These bands were found to change only between the δ_e and γ forms in the transition region of 70−120 °C. The bands at 601.9 and 607.6 cm^{-1} corresponding to the δ_e form decreased in the integrated absorbance drastically in the temperature region 70−100 °C. On further heating, the band positions shifted to 598.5 and 610 cm^{-1}, indicating that the structure changed to the γ form. After the structure changed to the γ form, the bands recovered more clearly and the integrated absorbance of these bands increased. The infrared bands observed in the temperature region 90−120 °C are a simple overlap of the bands of δ_e and γ forms. No bands intrinsic of the intermediate form appeared on the way of transition from δ_e to γ form, even when the infrared spectra were measured at a resolution power of 1 cm^{-1}. The total integrated absorbance in this frequency region was found to decrease drastically on the way of transition from δ_e to γ form and increased again when the structure changed to the γ form. Yoshioka et al.[15] measured the infrared spectra on the way of transition from δ to γ form for chloroform complex, and they did not observe such a kind of decrease in integrated absorbance during the δ to γ transition. These results clearly indicate that the T_2G_2 content is decreasing on the way of transition from the δ_e to γ form.

In this way, as long as we observe the phase transition from the viewpoint of infrared spectroscopy, we may say that no bands intrinsic of the intermediate form appeared on the way of transition from the δ_e to γ form. The transient decrease in the T_2G_2 content on the way of transition suggests that conformational disordering occurs during the transition process. The empty cavities present in the δ_e form seem to be responsible for such a behavior. When the cavities are erased during the transition process, the T_2G_2 content is decreased because of the conformational and chain-packing disorders due to the presence of cavities, and once all the cavities are erased completely, the T_2G_2 content is recovered, corresponding to the structural ordering into the γ form.

The DSC thermogram was investigated carefully on the δ_e form of sPS and chloroform complex. An endothermic peak followed by an exothermic peak is observed during the δ_e to γ phase transition in the temperature range 90−120 °C, as shown in Figure 9. At higher temperatures the γ form transforms to α form at 190−200 °C, and the melting of the α form occurs at around 265 °C. We need to remember that in Figure 3 the molecular chains keep the orientation almost perfectly during the phase transition. Therefore, the δ_e form is speculated to

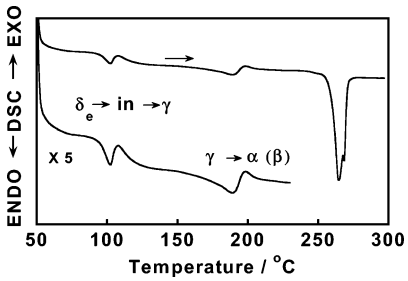

Figure 9. DSC thermogram of δ_e sample of sPS and chloroform complex taken in the heating process.

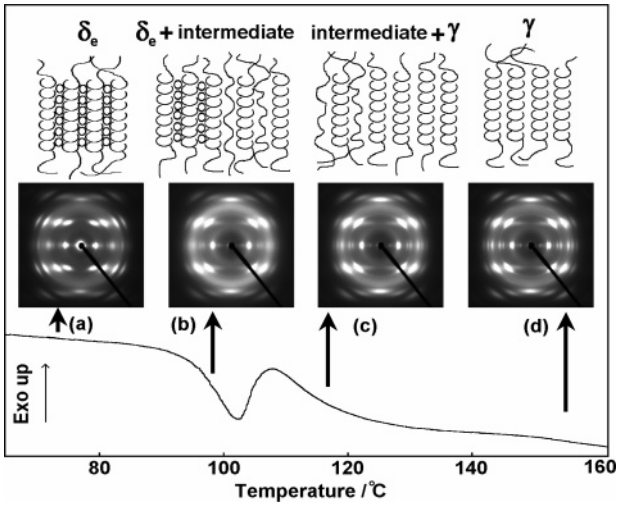

Figure 10. Schematic illustration of the chain-packing mode at different temperatures during heating of the δ_e form sample in comparison with the observed X-ray fiber diagram and DSC thermogram.

transform transiently to an intermediate phase with the conformationally disordered chains oriented along the draw axis, giving an endothermic peak in DSC thermogram, and then this intermediate phase transforms to the γ form by reorganizing the disordered chains, giving an exothermic peak in the DSC thermogram. These DSC results correspond well to the X-ray diffraction and infrared spectra data. The enthalpy change ΔH for δ_e to intermediate phase (endotherm) was estimated to be 96 J/mol, and the ΔH for intermediate phase to the γ form (exotherm) was found to be -95 J/mol from the DSC thermogram.

By combining the X-ray diffraction, infrared spectroscopy, and DSC results, we may speculate a phase transition model shown in Figure 10, where the X-ray fiber diagrams are also shown for comparison. Region (a) corresponds to the starting δ_e form where the T_2G_2 helical chains are packed with cavities inside the crystal lattice. In region (b), the δ_e and intermediate forms are coexistent, where the cavities start to decrease in the crystal lattice and the chain packing is disordered, corresponding to the endothermic peak in the DSC thermogram. The halo-like diffuse scatterings observed in the temperature regions (b) and (c) may originate from the disordered structure. As the temperature increases, the conformationally disordered chains gather together to form more tightly packed structure in region (c) and transforms to the γ phase finally (d). In the ordering process (c) the exothermic peak is observed in the DSC, and the T_2G_2 content is recovered as seen in the infrared spectral change.

Conclusions

In the present paper, we compared the X-ray fiber diagrams of the δ_e form of sPS with different solvent complexes like chloroform, toluene, and benzene. The X-ray fiber diagrams of the δ_e form were found to be different due to the difference in shape and volume of the cavities in the crystal lattice. But the infrared spectra are almost common to the δ_e forms with the different solvent cavities, as already pointed out by Yoshioka et al.[16] In the crystal lattice of the δ_e form, the polymer chains interact through cavities, and so the interactions are relatively weak compared with those in the γ form. The almost common infrared spectra of the δ_e form might result from such a situation. Contrarily, the infrared spectra of the δ form depend sensitively on the solvent type due to the interactions of polymer−solvent−polymer.

We measured the temperature dependence of the X-ray fiber diagram and polarized FTIR spectra starting from the uniaxially oriented δ_e form of sPS and chloroform complex at various temperatures. By combining all the experimental data of X-ray diffraction, infrared spectra, and DSC data collected during the phase transition, it has been found that the δ_e form transforms to the intermediate form transiently before transforming into the γ form. The DSC thermogram showed an endotherm followed by an exotherm. The X-ray reflections on the equatorial line are diffused during the phase transition from δ_e to γ, and the T_2G_2 content estimated from the infrared data is decreased. On the basis of such observations, it has been speculated that the intermediate form appeared during the phase transition is expected to take a disordered structure affected by the empty cavities present in the crystal lattice. That is to say, the rearrangement from the crystal lattice containing empty cavities to the closely packed crystal lattice requires the local disordering in the chain conformation as well as the chain-packing mode, corresponding to the intermediate phase. We are now analyzing the structure of these crystal forms based on the X-ray fiber diagram and computer simulation technique.

Acknowledgment. This work was financially supported by MEXT "Collaboration with Local Communities" Project (2005−2009). The authors thank Idemitsu Petrochemicals Co. Ltd., Japan, for supplying the sPS sample.

References and Notes

(1) Kobayashi, M.; Nakaoki, T.; Ishihara, N. *Macromolecules* **1989**, *22*, 4377−4382.
(2) Guerra, G.; Vitagliano, V. M.; De Rosa, C.; Petraccone, V.; Corradini, P. *Macromolecules* **1990**, *23*, 1539−1544.
(3) Woo, E. M.; Sun, Y. S.; Lee, M. L. *Polymer* **1999**, *40*, 4425−4429.
(4) Vittoria, V.; Filho, A. R.; De Candia, F. *J. Macromol. Sci., Phys.* **1990**, *B29*, 411−428.
(5) Cimmino, S.; Pace, E. Di.; Martuscelli, E.; Silvestre, C. *Polymer* **1991**, *32*, 1080−1083.
(6) De Rosa, C.; Rapacciuolo, M.; Guerra, G.; Petraccone, V. *Polymer* **1992**, *33*, 1423−1428.
(7) Woo, E. M.; Sun, Y. S.; Yang, C. P. *Prog. Polym. Sci.* **2001**, *26*, 945−983.
(8) Auriemma, F.; Petraccone, V.; Poggetto, F. D.; De Rosa, C.; Guerra, G.; Manfredi, C.; Corradini, P. *Macromolecules* **1993**, *26*, 3772−3777.
(9) Immirzi, A.; De Candia, F.; Iannelli, P.; Zambelli, A.; Vittoria, V. *Makromol. Chem. Rapid Commun.* **1988**, *9*, 761−764.
(10) Vittoria, V.; De Candia, F.; Iannelli, P.; Immirzi, A. *Makromol. Chem. Rapid Commun.* **1988**, *9*, 765−769.
(11) Manfredi, C.; De Rosa, C.; Guerra, G.; Rapacciuolo, M.; Auriemma, F.; Corradini, P. *Macromol. Chem. Phys.* **1995**, *196*, 2795−2808.
(12) Guadagno, L.; Baldi, P.; Vittoria, V.; Guerra, G. *Macromol. Chem. Phys.* **1998**, *199*, 2671−2675.
(13) Gowd, E. B.; Nair, S. S.; Ramesh, C. *Macromolecules* **2002**, *35*, 8509−8514.
(14) Gowd, E. B.; Nair, S. S.; Ramesh, C.; Tashiro, K. *Macromolecules* **2003**, *36*, 7388−7397.

(15) Yoshioka, A.; Tashiro, K. *Macromolecules* **2003**, *36*, 3593−3600.
(16) Yoshioka, A.; Tashiro, K. *Macromolecules* **2003**, *36*, 3001−3003.
(17) Ma, W.; Yu, J.; He, J. *Macromolecules* **2005**, *38*, 4755−4760.
(18) De Candia, F.; Romano, G.; Russo, R.; Vittoria, V. *Colloid Polym. Sci.* **1993**, *271*, 454−459.
(19) Ma, W.; Yu, J.; He, J. *Macromolecules* **2004**, *37*, 6912−6917.
(20) Rizzo, P.; Albunia, A. R.; Guerra, G. *Polymer* **2005**, *46*, 9549−9554.
(21) Vittoria, V.; Russo, R.; Candia, F. D. *Polymer* **1991**, *32*, 3371−3375.
(22) Tashiro, K.; Ueno, Y.; Yoshioka, A.; Kobayashi, M. *Macromolecules* **2001**, *34*, 310−315.
(23) Tashiro, K.; Yoshioka, A. *Macromolecules* **2002**, *35*, 410−414.
(24) Chatani, Y.; Shimane, Y.; Inoue, Y.; Inagaki, T.; Ishioka, T.; Ijitsu, T.; Yukinari, T. *Polymer* **1992**, *33*, 488−492.
(25) Rastogi, S.; Goossens, J. G. P.; Lemstra, P. J. *Macromolecules* **1998**, *31*, 2983−2998.
(26) Reynolds, N. M.; Hsu, S. L. *Macromolecules* **1990**, *23*, 3463−3472.
(27) Kobayashi, M.; Nakaoki, T.; Ishihara, N. *Macromolecules* **1990**, *23*, 78−83.
(28) Reynolds, N. M.; Stidham, H. D.; Hsu, S. L. *Macromolecules* **1991**, *24*, 3662−3665.
(29) Kellar, E. J. C.; Galiotis, C.; Andrews, E. H. *Macromolecules* **1996**, *29*, 3515−3520.
(30) Capitani, D.; De Rosa, C.; Ferrando, A.; Grassi, A.; Segre, A. L. *Macromolecules* **1992**, *25*, 3874−3880.
(31) Gomezls, M. A.; Tonelli, A. E. *Macromolecules* **1990**, *23*, 3385−3386.
(32) Tamai, Y.; Fukuda, M. *Macromol. Rapid Commun.* **2002**, *23*, 891−895.
(33) Reverchon, E.; Guerra, G.; Venditto, V. *J. Appl. Polym. Sci.* **1999**, *74*, 2077−2082.
(34) Rani, D. A.; Yamamoto, Y.; Mohri, S.; Sivakumar, M.; Tsujitha, Y.; Yoshimizu, H. *J. Polym. Sci., Part B: Polym. Phys.* **2003**, *41*, 269−273.
(35) Guerra, G.; Milano, G.; Venditto, V.; Musto, P.; De Rosa, C.; Cavallo, L. *Chem. Mater.* **2000**, *12*, 363−368.
(36) Milano, G.; Venditto, V.; Guerra, G.; Cavallo, L.; Ciambelli, P.; Sannino, D. *Chem. Mater.* **2001**, *13*, 1506−1511.
(37) Manfredi, C.; Guerra, G.; De Rosa, C.; Busico, V.; Corradini, P. *Macromolecules* **1995**, *28*, 6508−6515.
(38) De Rosa, C.; Guerra, G.; Petraccone, V.; Pirozzi, B. *Macromolecules* **1997**, *30*, 4147−4152.

MA061659D